

Pt-Ag Clusters and their Neutral Mononuclear Pt(II) Starting Complexes:
Structural and Luminescence Studies.

Juan Forniés*^a, Violeta Sicilia^{*b}, José M^a Casas^a, Antonio Martín^a, José A. López^a, Carmen Larraz^a, Pilar Borja^a and Carmen Ovejero^b

^aDepartamento de Química Inorgánica, Instituto de Ciencia de Materiales de Aragón, Facultad de Ciencias, Universidad de Zaragoza-CSIC, Plaza. S. Francisco s/n, 50009, Zaragoza, Spain.

E-mail: juan.fornies@unizar.es; Fax: +34 976-761159

^bDepartamento de Química Inorgánica, Instituto de Ciencia de Materiales de Aragón, Escuela Universitaria de Ingeniería Técnica Industrial, Universidad de Zaragoza-CSIC, Campus Universitario del Actur, Edificio Torres

Quevedo, 50018, Zaragoza, Spain. E-mail: sicilia@unizar.es; Fax: +34 976-762189

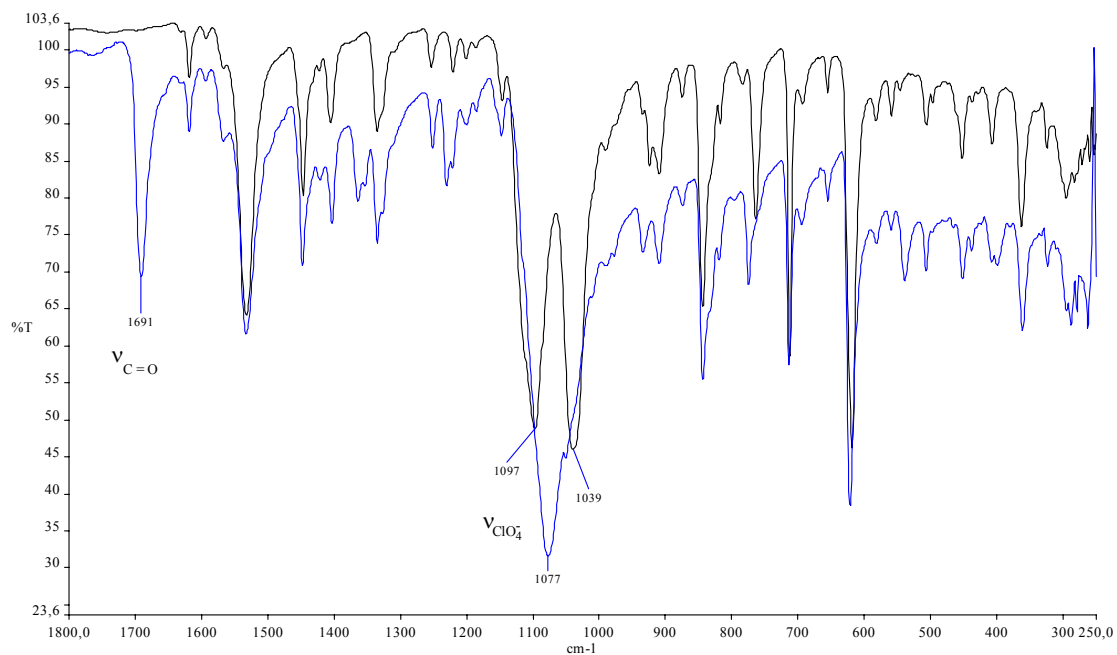


Figure S1. IR spectra of powdered solid (black) and crystals (blue) of compound **3**.

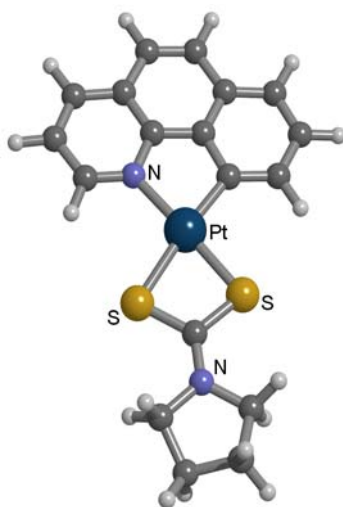
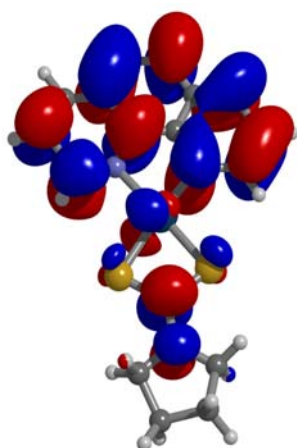


Figure S2.- DFT-Optimized structure of complex [Pt(bzq)(S₂CNC₄H₈)] (**1**)

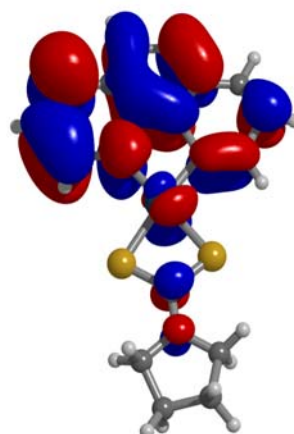
Table S1.- DFT-Optimized structure of complex **1**

Center	Coordinates (Å)		
	x	y	z
Pt	-0.01976	0.03119	-0.01015
S	1.71296	1.81858	-0.03754
S	1.75781	-0.74876	1.30148
N	-1.55192	0.78706	-1.17749
N	3.8063	0.99964	1.46211
C	-1.29656	-1.51551	0.12349
C	-1.19313	-2.72888	0.79332
H	-0.30288	-2.96385	1.36757
C	-2.23437	-3.67831	0.7443
H	-2.11578	-4.61446	1.28076
C	-3.39968	-3.44953	0.03296
H	-4.18818	-4.19384	0.00878
C	-3.55787	-2.23529	-0.66512
C	-4.72305	-1.89221	-1.43414
H	-5.53657	-2.60883	-1.48505
C	-4.82756	-0.70279	-2.09196
H	-5.71752	-0.46776	-2.66551
C	-3.76802	0.2656	-2.0434
C	-3.78649	1.51603	-2.68822
H	-4.64961	1.8079	-3.27686
C	-2.69989	2.36205	-2.56368
H	-2.6831	3.33035	-3.04707
C	-1.59617	1.96521	-1.79883
H	-0.73109	2.60493	-1.68243
C	-2.61892	-0.06163	-1.29073
C	-2.49959	-1.29843	-0.60115
C	2.59966	0.73422	0.97553
C	4.57298	0.07048	2.3148
H	4.55989	-0.93223	1.88433
H	4.11126	0.01844	3.30675

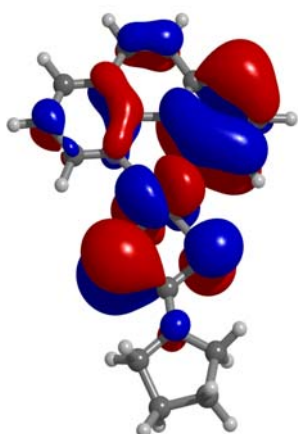
C	5.96994	0.70079	2.36285
H	6.56762	0.34829	1.51745
H	6.50324	0.44671	3.27982
C	5.68828	2.20515	2.22242
H	5.36844	2.62056	3.18234
H	6.55488	2.77411	1.88303
C	4.53306	2.2601	1.21686
H	3.86537	3.11085	1.35904
H	4.88925	2.28128	0.18133



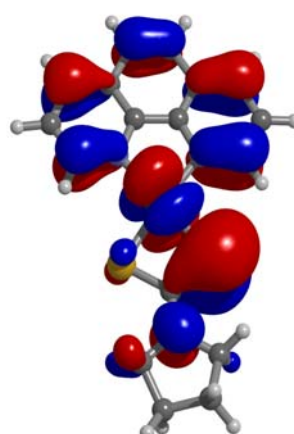
L+1 (96)



LUMO(95)



HOMO (94)



H-1 (93)

Figure S3. Representative frontier orbitals involved in the absorption of [Pt(bzq)(pdc)](1).

Table S2. Absorption data for compounds **1** and **2** in solutions 10^{-4} M at room temperature.

Compound	Solvent	$\lambda_{\text{abs}} / \text{nm} (10^3 \epsilon \text{ M}^{-1} \text{ cm}^{-1})$
1	Toluene	298 (13.7), 316 (15.8), 336 (14.2), 350 (13.2), 360 (12.3), 400 (12.7), 448 (1.7)
	2-MeTHF	308sh (9.3), 318 (12.4), 336 (12.1), 348sh (11.3), 360sh (10.3), 397 (10.3), 446 (1.3)
	CH ₂ Cl ₂	292sh (15.8), 308 (18.9), 320 (17.7), 332 (12.8), 350 (12.5), 391 (9.9), 444 (1.5)
	DMF	294sh (11.3), 312 (12.9), 332 (11.2), 350 (10.7), 364sh (7.5), 390 (8.8), 438 (1.4)
	NCMe	294sh (11.4), 308 (12.6), 328 (11.0), 348 (11.1), 386 (8.4), 434 (1.2)
2	Toluene	238(9.0), 246 (9.1), 256 (9.6), 264 (9.7), 276 (10.0), 298 (10.1), 318 (11.9), 338 (11.3), 350sh (10.6), 360 (9.7), 398 (9.8), 450 (1.2)
	2-MeTHF	240 (20.9), 256 (26.5), 274sh (8.1), 282 (6.4), 316 (11.2), 336 (11.2), 350sh (10.2), 360 (9.4), 397 (9.3), 448 (0.4)
	CH ₂ Cl ₂	222 (56.1), 238sh (56.1), 256 (34.1), 294 (11.8), 312 (12.7), 332 (12.1), 352 (11.9), 391 (9.3), 438 (1.9)
	DMF	292 (11.8), 310 (12.9), 332 (11.6), 350 (11.0), 390 (8.8), 436 (1.6)
	NCMe	220 (50.0), 236 (36.7), 252 (33.7), 290 (12.6), 308 (13.6), 330 (12.4), 348 (12.3), 354sh (11.1), 386 (9.1), 430 (1.8)

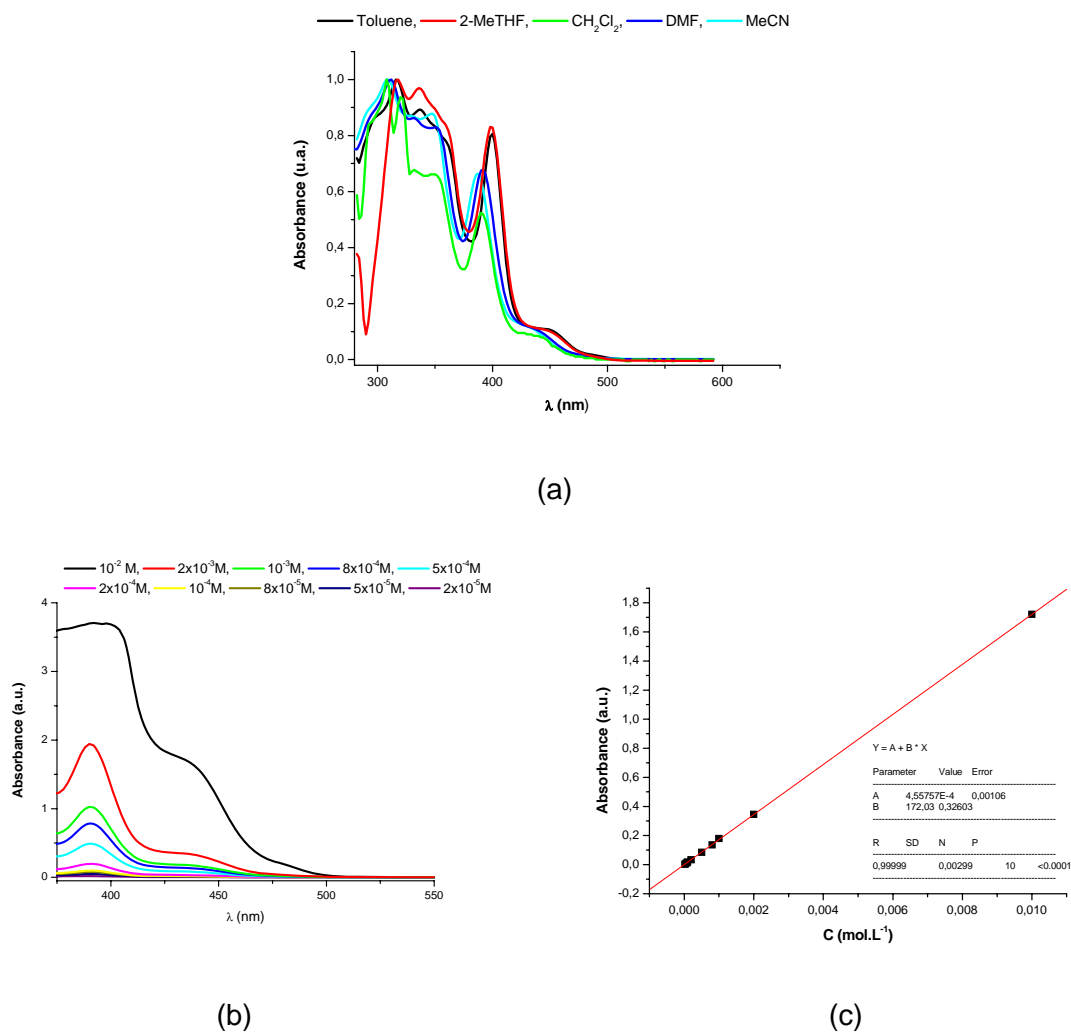


Figure S4. a) UV-visible absorption spectra of 1 in different solvents (10⁻⁴ M) showing negative solvatochromism. b) Expansion of the low-energy region of the UV-visible spectra of 1 in CH₂Cl₂ at 298K at different concentrations. c) Representation of the linear fit of the absorbance at 444 nm (A_{444}) vs. concentration.

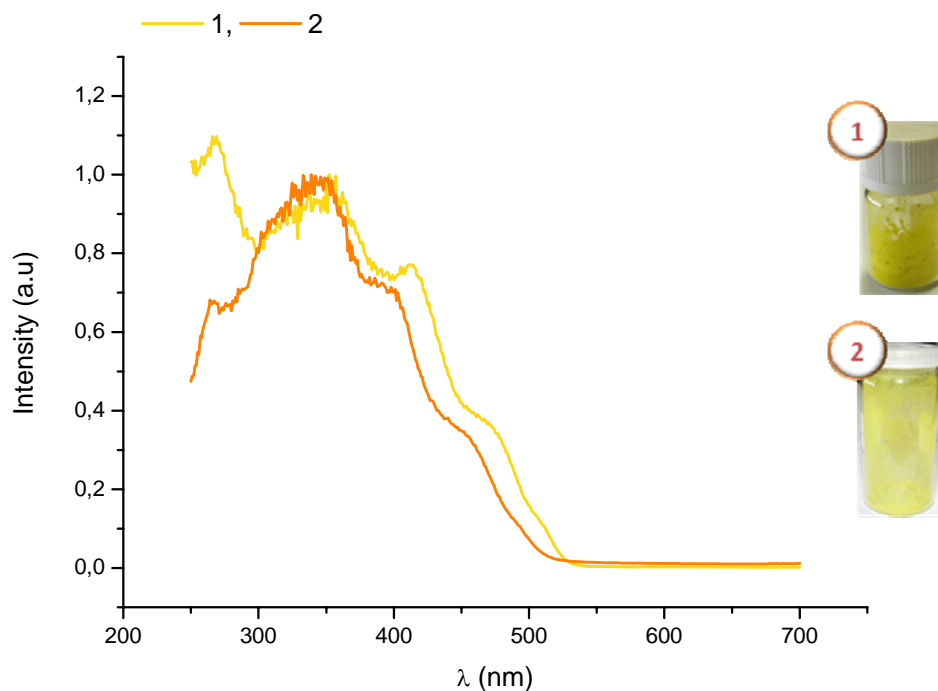


Figure S5. Normalized Diffuse Reflectance UV-vis (DRUV) spectra of **1** and **2** in solid state at room temperature.

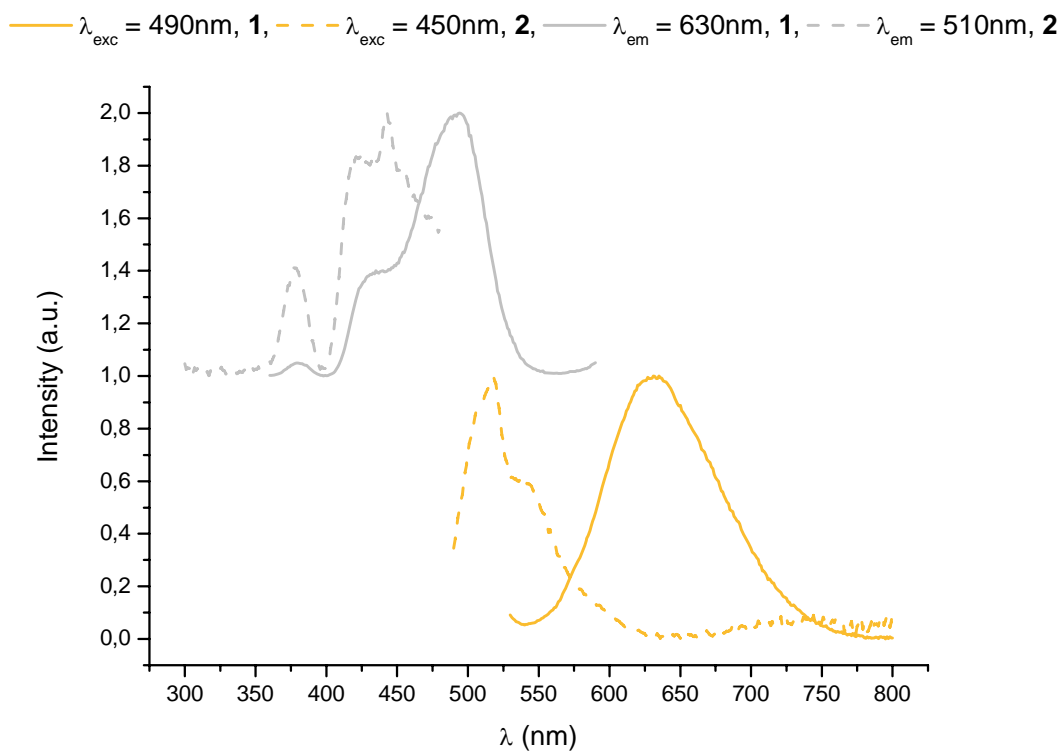


Figure S6. Normalized emission and excitation spectra of **1** and **2** in 2-Me-THF (10^{-3} M) at 298 K

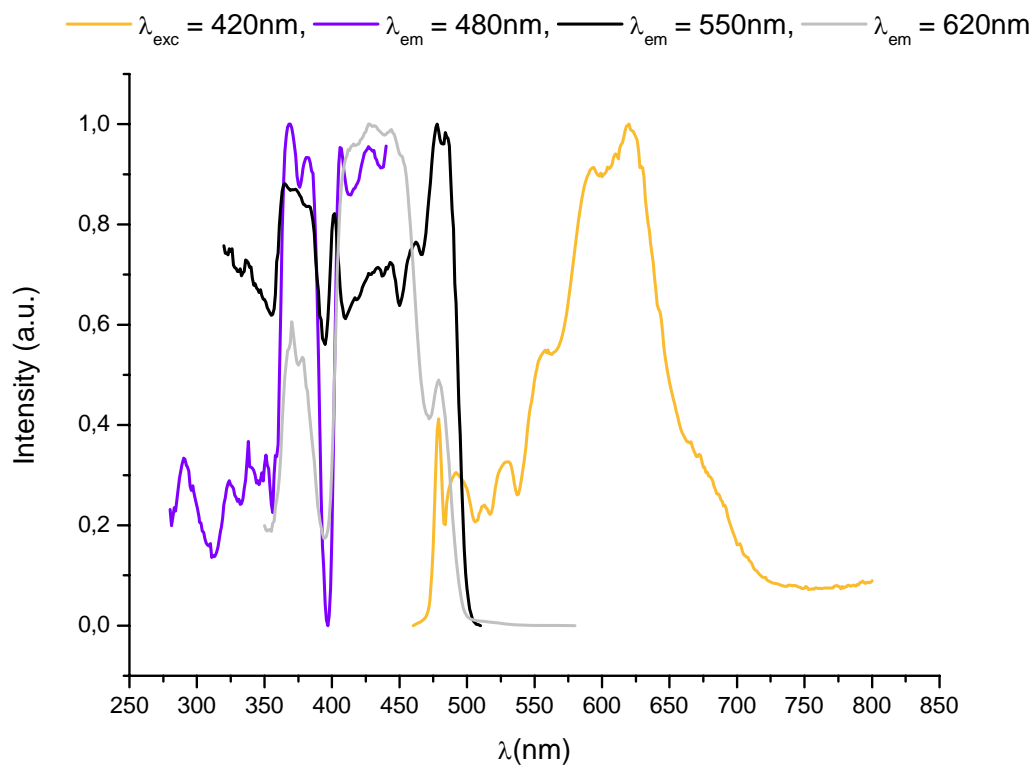


Figure S7. Normalized emission and excitation spectra of **1** in 2-Me-THF (10^{-3} M) at 77 K.

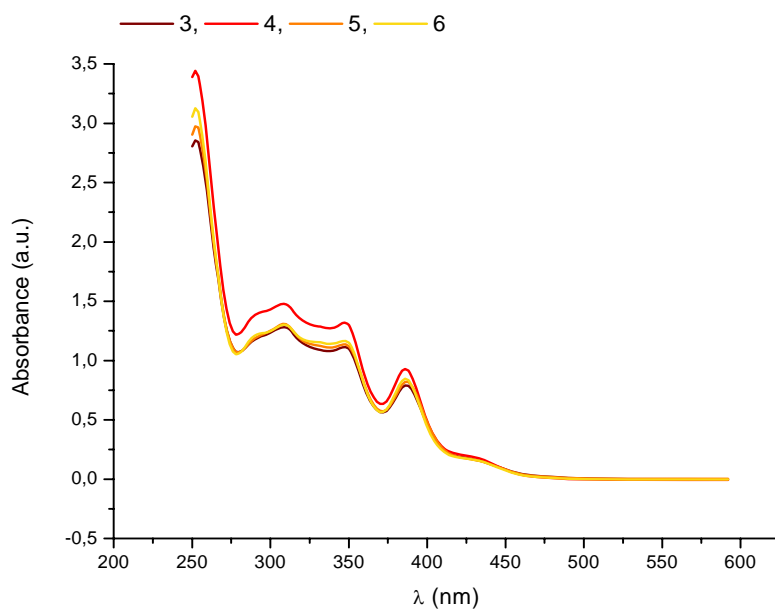


Figure S8. Absorption spectra of compounds **3-6** in acetonitrile solution 5×10^{-4} M

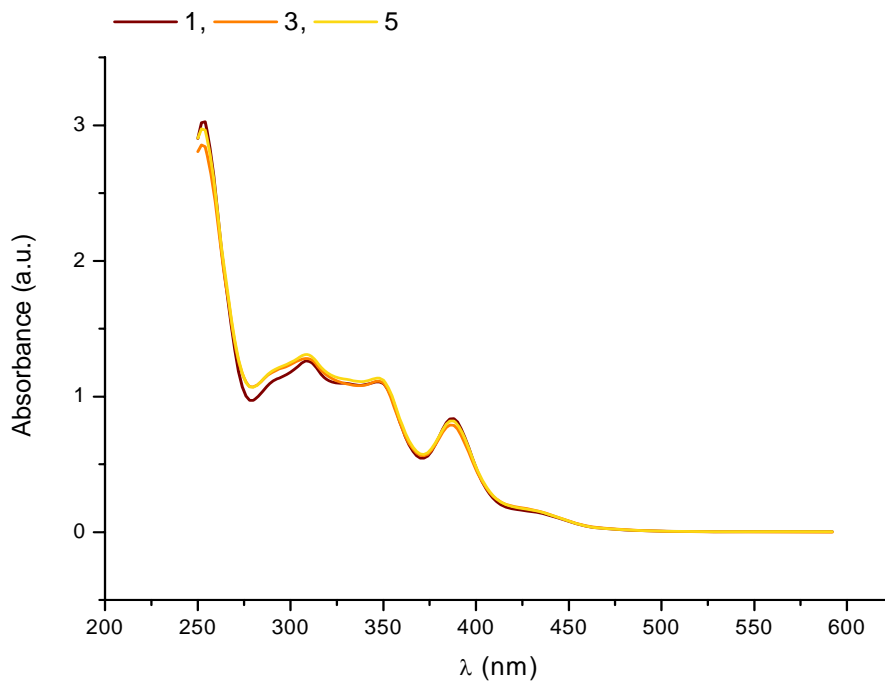


Figure S9 . Absorption spectra in acetonitrile solution of **1** (10^{-4} M), **3** (5×10^{-4} M) and **5** (5×10^{-4} M) at room temperature.

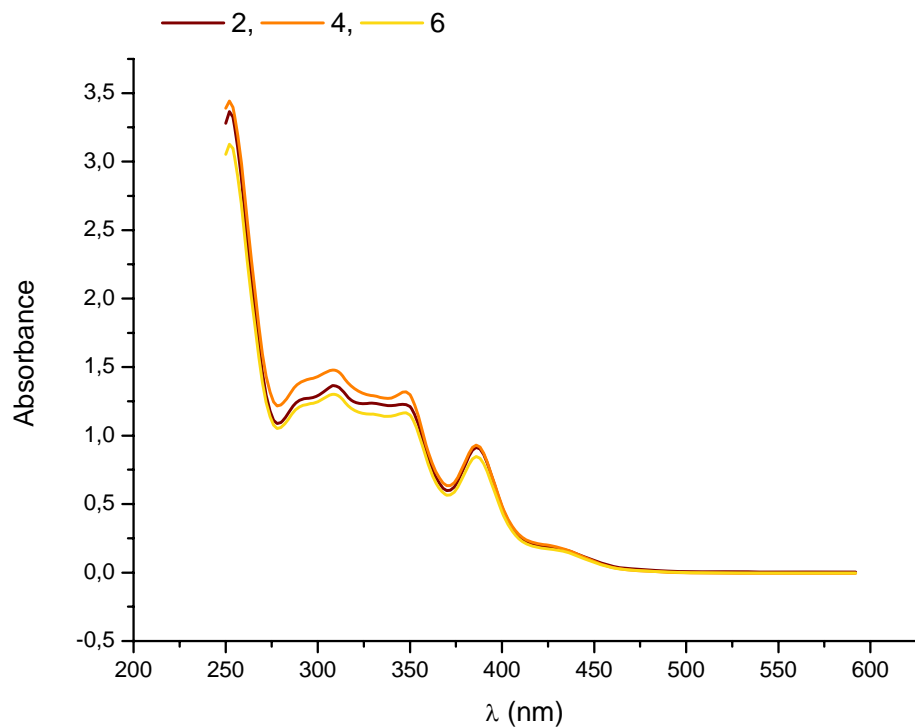


Figure S10. Absorption spectra in acetonitrile solution of **2** (10^{-4} M), **4** (5×10^{-4} M) and **6** (5×10^{-4} M) at room temperature.

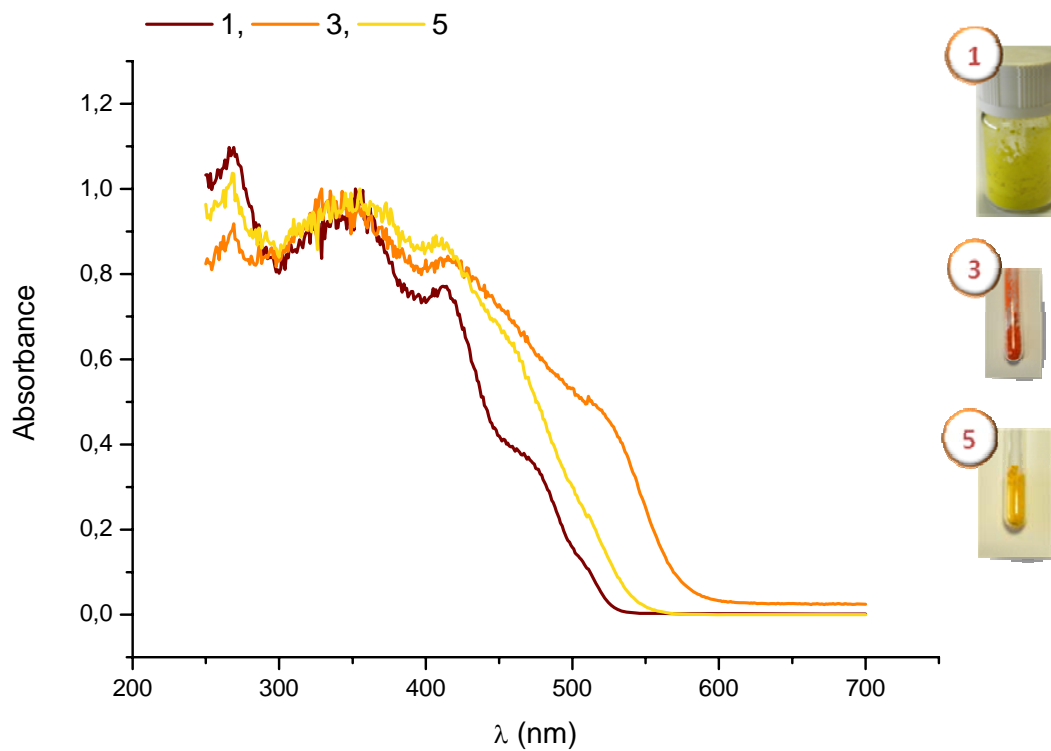


Figure S11. Normalized Diffuse Reflectance UV-vis (DRUV) spectra of **1**, **3**, **5** in solid state.

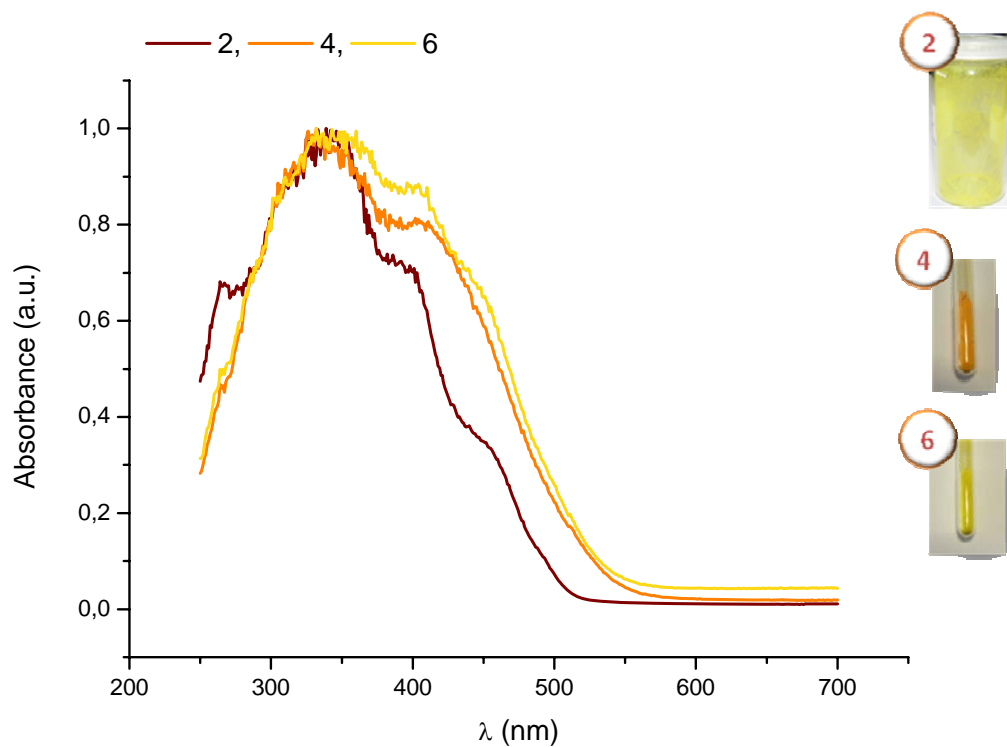


Figure S12. Normalized Diffuse Reflectance UV-vis (DRUV) spectra of compounds **2**, **4**, **6** in solid

state.

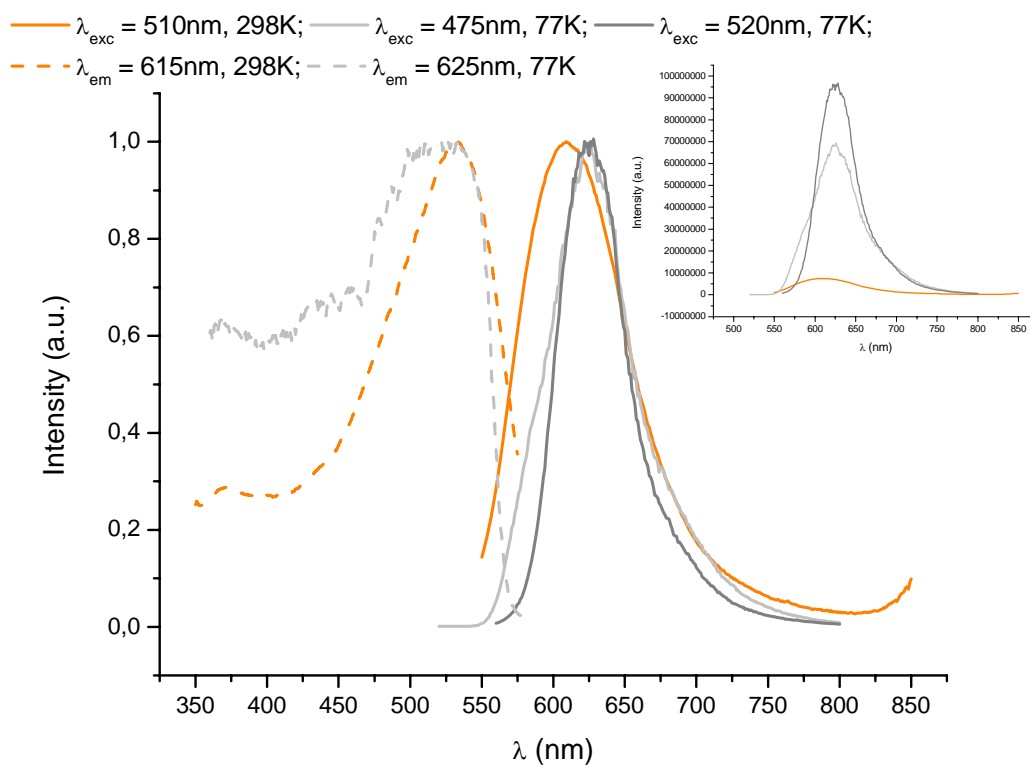


Figure S13. Normalized excitation and emission spectra of **4** in the solid state at 298K (Orange) and 77 K(Grey). Inset: Unnormalized spectra.

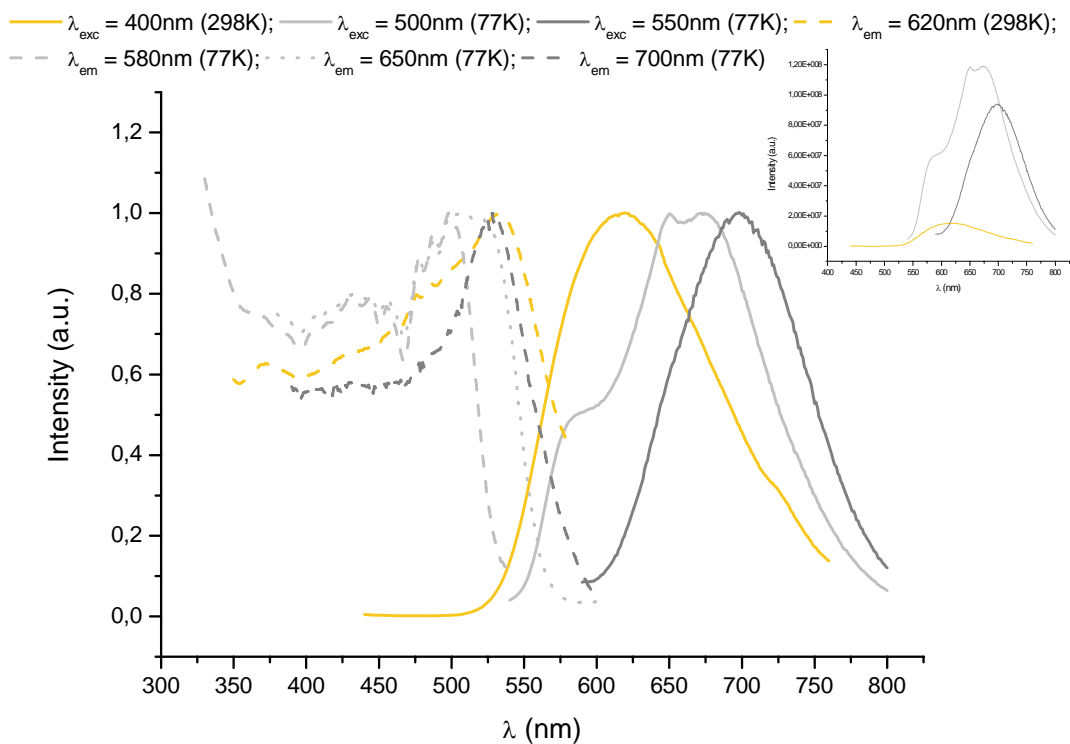


Figure S14. Normalized excitation and emission spectra of **5** in the solid state at 298K (yellow) and 77K (Grey). Inset: Unnormalized spectra.

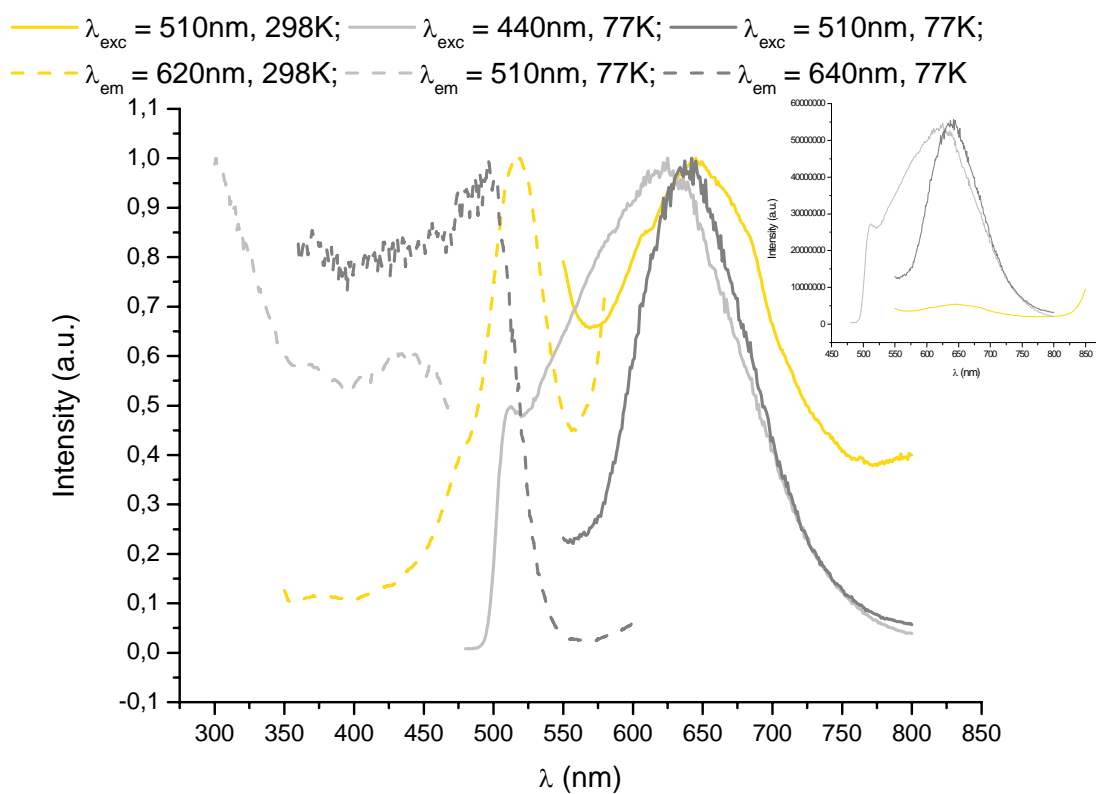


Figure S15. Normalized excitation and emission spectra of **6** in the solid state at 298K (yellow) and 77K (grey). Inset: Unnormalized emission spectra.

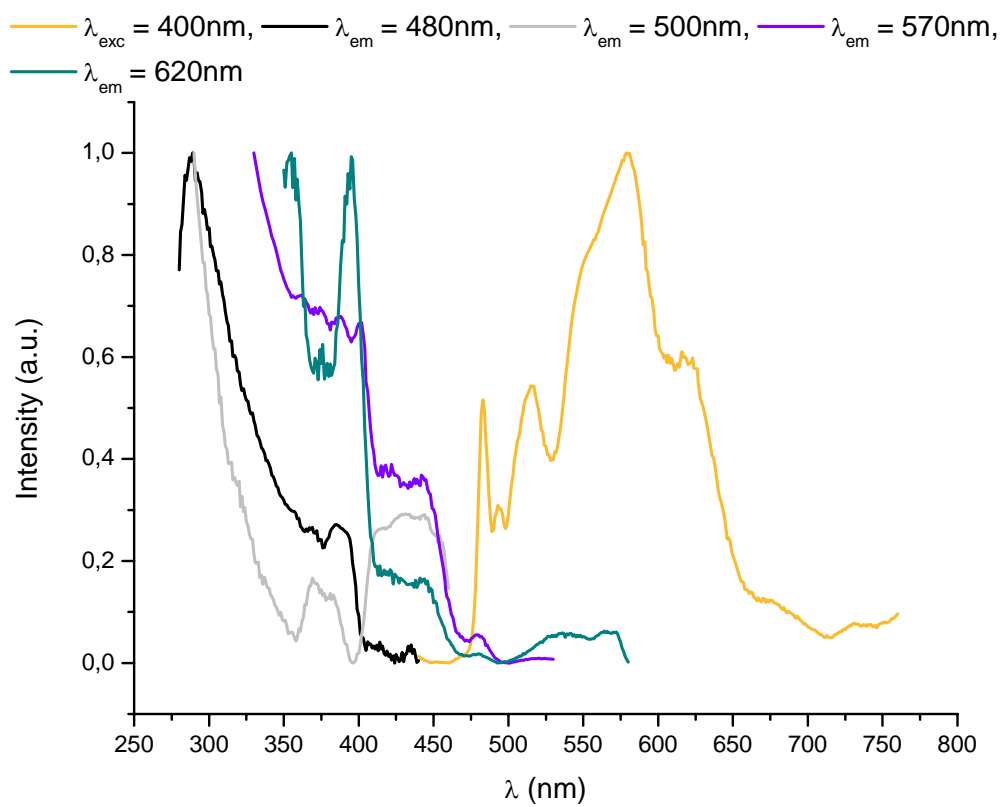


Figure S16. Normalized emission and excitation spectra of a saturated solution of **3** in 2-Me-THF at 77K .

Experimental Section

Full IR and NMR data of complexes 1-6

[Pt(bzq)(pdtc)] (1): IR data, ν_{\max} (cm^{-1}): 1615 m, 1564 m, 1508 vs ($\nu_{\text{C-N}}$), 1443 vs, 1398 s, 1326 s, 1164 m, 940 m ($\nu_{\text{C-S}}$), 825 vs, 815 vs, 750 s, 710 vs, 365 s ($\nu_{\text{Pt-S}}$), 310 s ($\nu_{\text{Pt-S}}$). ^1H NMR (400 MHz, CD_2Cl_2 , 298 K) δ_{H} : 8.81 (1H, dd, $^3J_{2,3} = 5.2$ Hz, $^4J_{2,4} = 1.2$ Hz, $^3J_{\text{Pt-H}} = 40.4$ Hz, 2-H bzq), 8.40 (1H, dd, $^4J_{4,2} = 1.2$ Hz, $^3J_{4,3} = 8.1$ Hz, 4-H bzq), 7.81 (1H, AB, $^3J_{5,6} = 8.8$ Hz, 5-H bzq), 7.65 (1H, dd, $^3J_{7,8} = 7.8$ Hz, $^4J_{7,9} = 0.9$ Hz, 7-H bzq), 7.62 (1H, AB, $^3J_{6,5} = 8.8$ Hz, 6-H bzq), 7.47 (2H, m, 3-H, 8-H bzq), 7.42 (1H, dd, $^4J_{9,7} = 0.9$ Hz, $^3J_{9,8} = 7.0$ Hz, $^3J_{\text{Pt-H}} = 48$ Hz, 9-H bzq), 3.90 (4H, m, CH_2^{a}), 2.10 (4H, m, CH_2^{b}) ppm. ^1H NMR (300 MHz, Acetonitrile- d^3 , 298 K) δ_{H} : 8.86 (1H, dd, $^3J_{2,3} = 5.3$ Hz, $^4J_{2,4} = 1.2$ Hz, $^3J_{\text{Pt-H}} = 39.4$ Hz, 2-H bzq), 8.54 (1H, dd, $^4J_{4,2} = 1.2$ Hz, $^3J_{4,3} = 8.1$ Hz, 4-H bzq), 7.86 (1H, AB, $^3J_{5,6} = 8.8$ Hz, 5-H bzq), 7.72 (1H, AB, $^3J_{6,5} = 8.8$ Hz, 6-H bzq), 7.68 (1H, dd, $^3J_{7,8} = 7.8$ Hz, $^4J_{7,9} = 0.8$ Hz, 7-H bzq), 7.55 (1H, dd, $^3J_{3,2} = 5.3$ Hz, $^3J_{3,4} = 8.1$ Hz, 3-H bzq), 7.48 (1H, dd, $^3J_{8,7} = 7.8$ Hz, $^4J_{8,9} = 7.2$ Hz, 8-H bzq), 7.37 (1H, dd, $^3J_{9,7} = 0.8$ Hz, $^4J_{9,8} = 7.2$ Hz, $^3J_{\text{Pt-H}} = 55.4$ Hz, 9-H bzq), 3.87 (4H, m, CH_2^{a}), 2.10 (4H, m, CH_2^{b} overlapped with solvent signals) ppm. ^{13}C NMR (100.58 MHz, CD_2Cl_2 , 298K) δ_{C} : 149.00 (s, $^2J_{\text{Pt-C}} = 34.6$ Hz, 2-C bzq), 144.15 (s), 137.15 (s, 4-C bzq), 134.21 (s), 130.28 (s, 3-C bzq), 130.20 (s, 8-C bzq), 129.78 (s, 5-C bzq), 127.42 (s), 123.53 (s, 6-C bzq), 122.27 (s, $^2J_{\text{Pt-C}} = 37.1$ Hz, 9-C bzq), 121.40 (7-C bzq), 50.78 (s), 50.10 (s), 25.08 (s), 24.93 (s) ppm;

[Pt(bzq)(dmdtc)] (2): IR data, ν_{\max} (cm^{-1}): 1618 m, 1543 vs ($\nu_{\text{C-N}}$), 1446 s, 1397 vs, 1328 s, 1244 m, 1155 s, 1135 s, 963 s ($\nu_{\text{C-S}}$), 821 s, 810 vs, 738 s, 707 vs, 502 m, 436 s, 382 m ($\nu_{\text{Pt-S}}$), 320 m ($\nu_{\text{Pt-S}}$). ^1H NMR (400 MHz, CD_2Cl_2 , 298 K) δ_{H} : 8.82 (1H, dd, $^3J_{2,3} = 5.2$ Hz, $^4J_{2,4} = 1.3$ Hz, $^3J_{\text{Pt-H}} = 39.6$ Hz, 2-H bzq), 8.40 (1H, dd, $^4J_{4,2} = 1.3$ Hz, $^3J_{4,3} = 8.1$ Hz, 4-H bzq), 7.81 (1H, AB, $^3J_{5,6} = 8.7$ Hz, 5-H bzq), 7.65 (1H, dd, $^3J_{7,8} = 7.7$ Hz,

$^4J_{7,9} = 1.0$ Hz, 7-H *bzq*), 7.62 (1H, AB, $^3J_{6,5} = 8.7$ Hz, 6-H *bzq*), 7.48 (3H, m, 3-H, 8-H, 9-H *bzq*), 3.40 (3H, s, CH₃), 3.39 (3H, s, CH₃) ppm. ^1H NMR (300 MHz, Acetonitrile-*d*³, 298 K) δ_{H} : 8.86 (1H, dd, $^3J_{2,3} = 5.2$ Hz, $^4J_{2,4} = 1.3$ Hz, $^3J_{\text{Pt-H}} = 39.6$ Hz, 2-H *bzq*), 8.54 (1H, dd, $^4J_{4,2} = 1.3$ Hz, $^3J_{4,3} = 8.1$ Hz, 4-H *bzq*), 7.86 (1H, AB, $^3J_{5,6} = 8.8$ Hz, 5-H *bzq*), 7.72 (1H, AB, $^3J_{6,5} = 8.8$ Hz, 6-H *bzq*), 7.68 (1H, dd, $^3J_{7,8} = 7.9$ Hz, $^4J_{7,9} = 0.9$ Hz, 7-H *bzq*), 7.56 (1H, dd, $^3J_{3,2} = 5.2$ Hz, $^3J_{3,4} = 8.1$ Hz, 3-H *bzq*), 7.51 (1H, dd, $^3J_{8,7} = 7.8$ Hz, $^4J_{8,9} = 7.0$ Hz, 8-H *bzq*), 7.39 (1H, dd, $^3J_{9,7} = 0.9$ Hz, $^4J_{9,8} = 7.0$ Hz, $^3J_{\text{Pt-H}} = 55.1$ Hz, 9-H *bzq*), 3.38 (3H, s, CH₃), 3.37 (3H, s, CH₃) ppm. ^{13}C NMR (75.43 MHz, CD₂Cl₂, 298K) δ_{C} : 148.68 (s, $^2J_{\text{Pt-C}} = 34.3$ Hz, 2-C *bzq*), 144.25 (s), 136.85 (s, 4-C *bzq*), 133.87 (s), 129.94 (s, 3-C *bzq*), 129.70 (s, 8-H *bzq*), 129.45 (s, 5-C *bzq*), 127.08 (s), 123.16 (s, 6-C *bzq*), 121.89 (s, $^2J_{\text{Pt-C}} = 37.9$ Hz, 9-C *bzq*), 121.08 (7-C *bzq*), 38.99 (s), 40.08 (s) ppm.

[{Pt(*bzq*)(*pdtc*)}₂Ag₂](ClO₄)₂ (3): IR data, ν_{max} (cm⁻¹): 1618 w, 1531 s ($\nu_{\text{C-N}}$), 1446 m, 1405 m, 1335 m, 1097 vs (ClO₄⁻), 1039 vs (ClO₄⁻), 923 m, 909 m, 843 m, 763 m, 712 s, 618 vs (ClO₄⁻), 362 m ($\nu_{\text{Pt-S}}$). ^1H NMR (300 MHz, Acetonitrile-*d*³, 298 K) δ_{H} : 8.68 (2H, m, $^3J_{\text{Pt-H}} = 40.5$ Hz, 2-H *bzq*), 8.49 (2H, dd, $^4J_{4,2} = 0.9$ Hz, $^3J_{4,3} = 8.1$ Hz, 4-H *bzq*), 7.82 (2H, AB, $^3J_{5,6} = 8.8$ Hz, 5-H *bzq*), 7.68 (4H, 6-H *bzq* (AB), 7-H *bzq*), 7.51 (2H, dd, $^3J_{3,2} = 5.3$ Hz, $^3J_{3,4} = 8.1$ Hz, 3-H *bzq*), 7.44 (2H, dd, $^3J_{8,7} = 7.9$ Hz, $^4J_{8,9} = 7.1$ Hz, 8-H *bzq*), 7.28 (2H, d, $^4J_{9,8} = 7.1$ Hz, $^3J_{\text{Pt-H}} = 55.2$ Hz, 9-H *bzq*), 3.75 (8H, m, CH₂^a), 2.03 (8H, m, CH₂^b overlapped with solvent signals) ppm.

[{Pt(*bzq*)(*dmdtc*)}₂Ag₂](ClO₄)₂ (4): IR data, ν_{max} (cm⁻¹): 1620 w, 1575 s ($\nu_{\text{C-N}}$), 1449 m, 1405 s, 1080 vs (ClO₄⁻), 832 s, 815 m, 762 m, 709 s, 620 vs (ClO₄⁻), 435 m, 386 m ($\nu_{\text{Pt-S}}$), 330 m ($\nu_{\text{Pt-S}}$). ^1H NMR (300 MHz, Acetonitrile-*d*³, 298 K) δ_{H} : 8.74 (2H, dd, $^3J_{2,3} = 5.1$ Hz, $^4J_{2,4} = 0.9$ Hz, $^3J_{\text{Pt-H}} = 39.1$ Hz, 2-H *bzq*), 8.51 (2H, dd, $^4J_{4,2} = 0.9$ Hz, $^3J_{4,3} = 8.2$ Hz, 4-H *bzq*), 7.83 (2H, AB, $^3J_{5,6} = 8.8$ Hz, 5-H *bzq*), 7.70 (2H, AB, $^3J_{6,5} = 8.8$ Hz,

6-H *bzq*), 7.68 (2H, dd, $^3J_{7,8} = 7.9$ Hz, $^4J_{7,9} = 0.7$ Hz, 7-H *bzq*), 7.54 (2H, dd, $^3J_{3,2} = 5.2$ Hz, $^3J_{3,4} = 8.1$ Hz, 3-H *bzq*), 7.48 (2H, dd, $^3J_{8,7} = 7.9$ Hz, $^4J_{8,9} = 7.1$ Hz, 8-H *bzq*), 7.32 (2H, dd, $^3J_{9,7} = 0.7$ Hz, $^4J_{9,8} = 7.1$ Hz, $^3J_{\text{Pt-H}} = 53.5$ Hz, 9-H *bzq*), 3.34 (6H, s, CH₃), 3.31 (6H, s, CH₃) ppm.

[{Pt(*bzq*)(*pdtc*)}₂Ag]ClO₄ (5): IR data, ν_{max} (cm⁻¹): 1618 w, 1522 s ($\nu_{\text{C-N}}$), 1447 s, 1403 m, 1331 m, 1080 vs (ClO₄⁻), 935 m ($\nu_{\text{C-S}}$), 910 m, 831 vs, 816 m, 762 m, 711 vs, 621 vs (ClO₄⁻), 369 m ($\nu_{\text{Pt-S}}$), 303 m ($\nu_{\text{Pt-S}}$). ¹H NMR, (400 MHz, CD₂Cl₂, 298 K) δ_{H} : 8.26 (2H, d, $^3J_{2,3} = 4.7$ Hz, $^3J_{\text{Pt-H}} = 39.1$ Hz, 2-H *bzq*), 8.08 (2H, d, $^3J_{4,3} = 8.3$ Hz, 4-H *bzq*), 7.61 (2H, AB, $^3J_{5,6} = 8.8$ Hz, 5-H *bzq*), 7.50 (2H, d, $^3J_{7,8} = 7.9$ Hz, 7-H *bzq*), 7.40 (2H, AB, $^3J_{6,5} = 8.8$ Hz, 6-H *bzq*), 7.15 (2H, m, 8-H *bzq*), 7.03 (4H, m, 3-H, 9-H *bzq*), 3.84 (8H, m, CH₂^a), 2.07 (8H, m, CH₂^b) ppm. ¹H NMR (300 MHz, Acetonitrile-d₃, 298 K) δ_{H} : 8.79 (2H, dd, $^3J_{2,3} = 5.3$ Hz, $^4J_{2,4} = 1.0$ Hz, $^3J_{\text{Pt-H}} = 40.2$ Hz, 2-H *bzq*), 8.52 (2H, dd, $^4J_{4,2} = 1.0$ Hz, $^3J_{4,3} = 8.1$ Hz, 4-H *bzq*), 7.84 (2H, AB, $^3J_{5,6} = 8.8$ Hz, 5-H *bzq*), 7.70 (2H, AB, $^3J_{6,5} = 8.8$ Hz, 6-H *bzq*), 7.67 (2H, dd, $^3J_{7,8} = 7.9$ Hz, $^4J_{7,9} = 0.8$ Hz, 7-H *bzq*), 7.54 (2H, dd, $^3J_{3,2} = 5.3$ Hz, $^3J_{3,4} = 8.1$ Hz, 3-H *bzq*), 7.46 (2H, dd, $^3J_{8,7} = 7.9$ Hz, $^4J_{8,9} = 7.1$ Hz, 8-H *bzq*), 7.34 (2H, dd, $^3J_{9,7} = 0.8$ Hz, $^4J_{9,8} = 7.1$ Hz, $^3J_{\text{Pt-H}} = 55.3$ Hz, 9-H *bzq*), 3.82 (8H, m, CH₂^a), 2.06 (8H, m, CH₂^b overlapped with solvent signals) ppm.

[{Pt(*bzq*)(*dmdtc*)}₂Ag]ClO₄ (6): IR data, ν_{max} (cm⁻¹): 1618 m, 1554 s ($\nu_{\text{C-N}}$), 1447 m, 1401 s, 1331 m, 1241 m, 1080 vs (ClO₄⁻), 949 m ($\nu_{\text{C-S}}$), 831 vs, 816 m, 760 m, 712 vs, 622 vs (ClO₄⁻), 434 m, 387 m ($\nu_{\text{Pt-S}}$), 327 m ($\nu_{\text{Pt-S}}$); ¹H NMR (300 MHz, Acetonitrile-d₃, 298 K) δ_{H} : 8.76 (2H, dd, $^3J_{2,3} = 5.1$ Hz, $^4J_{2,4} = 0.8$ Hz, $^3J_{\text{Pt-H}} = 39.8$ Hz, 2-H *bzq*), 8.51 (2H, dd, $^4J_{4,2} = 0.8$ Hz, $^3J_{4,3} = 8.1$ Hz, 4-H *bzq*), 7.83 (2H, AB, $^3J_{5,6} = 8.8$ Hz, 5-H *bzq*), 7.70 (2H, AB, $^3J_{6,5} = 8.8$ Hz, 6-H *bzq*), 7.67 (2H, dd, $^3J_{7,8} = 7.8$ Hz, $^4J_{7,9} = 0.8$ Hz, 7-H *bzq*), 7.53 (2H, dd, $^3J_{3,2} = 5.2$ Hz, $^3J_{3,4} = 8.1$ Hz, 3-H *bzq*), 7.48 (2H, dd, $^3J_{8,7} = 7.8$ Hz,

$^4J_{8,9} = 7.1$ Hz, 8-H *bzq*), 7.34 (2H, dd, $^3J_{9,7} = 0.8$ Hz, $^4J_{9,8} = 7.1$ Hz, $^3J_{\text{Pt-H}} = 54.5$ Hz 9-H *bzq*), 3.34 (6H, s, CH₃), 3.32 (6H, s, CH₃) ppm.

General procedures and materials. The starting material [Pt(*bzq*)(NCMe₂)₂]₂ClO₄¹ was prepared as described elsewhere. Ammonium pyrrolidinedithiocarbamate (NH₄S₂CNC₄H₈), sodium dimethyldithiocarbamate dihydrate (NaS₂CNMe₂·2H₂O), and silver perchlorate (AgClO₄) were purchased from commercial suppliers. Elemental analyses were carried out with a Perkin Elmer 2400 CHNS analyzer. IR spectra were recorded on a Perkin-Elmer Spectrum 100 FT-IR Spectrometer (ATR in the range 250-4000 cm⁻¹). Mass spectral analyses were performed with a Microflex MALDI-TOF Bruker or an Autoflex III MALDI-TOF Bruker instruments. NMR spectra were recorded on a Bruker 300 or 400 spectrometer using the standard references: SiMe₄ for ¹H and ¹³C. All of the ¹³C were proton-decoupled, *J* are given in Hz and assignments are based on ¹H-¹H COSY and ¹H-¹³C g-HSQC experiments. UV-visible spectra were obtained on a Thermo electron corporation evolution 600 spectrometer. Diffuse reflectance UV-vis (DRUV) spectra were recorded on a Thermo electron corporation evolution 600 spectrophotometer equipped with a Praying Mantis integrating sphere. The solid samples were homogeneously diluted with silica. The mixtures were placed in a homemade cell equipped with quartz window. Steady-state photoluminescence spectra were recorded on a Jobin-Yvon Horiba Fluorolog FL-3-11 Tau 3 spectrofluorimeter using band pathways of 3 nm for both excitation and emission. Phosphorescence lifetimes were recorded with a Fluoromax phosphorimeter accessory containing a UV xenon flash tube with a flash rate between 0.05 and 25 Hz. Phase shift and modulation were recorded over the frequency range of 0.1-100 MHz. Nanosecond lifetimes were recorded with an IBH 5000F Coaxial nanosecond flahlamp. The lifetime data were fitted using the Jobin-Yvon software package and the Origin Pro 8 program.

Computational Details. The computational method used was density functional theory (DFT) with the B3LYP exchange-correlation functional,²⁻⁴ using the Gaussian 03⁵ program package. The basic set used was the LanL2DZ effective core potential for the platinum atom, and 6-31G(d,p) for the remaining atoms. Time-dependent density-functional theory (TD-DFT) calculation were carried out using the polarized continuum model approach implemented in the Gaussian 03 software.

References

- (1) Forniés, J.; Fuertes, S.; López, J. A.; Martín, A.; Sicilia, V. *Inorg. Chem.* **2008**, *47*, 7166.
- (2) Becke, A. D. *Phys. Rev. A: At., Mol., Opt. Phys.* **1988**, *38*, 3098.
- (3) Lee, C.; Yang, W.; Parr, R. G. *Phys. Rev. B: Condens. Matter Mater. Phys.* **1988**, *37*, 785.
- (4) Becke, A. D. *J. Chem. Phys.* **1993**, *98*, 5648.
- (5) Gaussian 03, Revision E.01, M. J. Frisch, G. W. Trucks, H. B. Schlegel, G. E. Scuseria, M. A. Robb, J. R. Cheeseman, J. A. Montgomery, Jr., T. Vreven, K. N. Kudin, J. C. Burant, J. M. Millam, S. S. Iyengar, J. Tomasi, V. Barone, B. Mennucci, M. Cossi, G. Scalmani, N. Rega, G. A. Petersson, H. Nakatsuji, M. Hada, M. Ehara, K. Toyota, R. Fukuda, J. Hasegawa, M. Ishida, T. Nakajima, Y. Honda, O. Kitao, H. Nakai, M. Klene, X. Li, J. E. Knox, H. P. Hratchian, J. B. Cross, V. Bakken, C. Adamo, J. Jaramillo, R. Gomperts, R. E. Stratmann, O. Yazyev, A. J. Austin, R. Cammi, C. Pomelli, J. W. Ochterski, P. Y. Ayala, K. Morokuma, G. A. Voth, P. Salvador, J. J. Dannenberg, V. G. Zakrzewski, S. Dapprich, A. D. Daniels, M. C. Strain, O. Farkas, D. K. Malick, A. D. Rabuck, K. Raghavachari, J. B. Foresman, J. V. Ortiz, Q. Cui, A. G. Baboul, S. Clifford,

J. Cioslowski, B. B. Stefanov, G. Liu, A. Liashenko, P. Piskorz, I. Komaromi, R. L. Martin, D. J. Fox, T. Keith, M. A. Al-Laham, C. Y. Peng, A. Nanayakkara, M. Challacombe, P. M. W. Gill, B. Johnson, W. Chen, M. W. Wong, C. Gonzalez, and J. A. Pople, Gaussian, Inc., Wallingford CT, 2004.